Laser ablation source for formation and deposition of size-selected metal clusters

Vuckovic, Sasa; Svanqvist, M.; Popok, Vladimir

Published in:
Review of Scientific Instruments

DOI (link to publication from Publisher):
10.1063/1.2952503

Publication date:
2008

Document Version
Publisher's PDF, also known as Version of record

Laser ablation source for formation and deposition of size-selected metal clusters

S. Vučković,[a] M. Svanqvist,[b] and V. N. Popok
Department of Physics, Göteborg University, SE-412 96 Göteborg, Sweden

(Received 5 May 2008; accepted 8 June 2008; published online 1 July 2008)

This work describes construction of a source and optimisation of its parameters for production of cluster ion beams using material ablation by the second harmonic of a Nd:YAG laser (532 nm). The influence of different source parameters such as carrier gas pressure, laser power, delay time between gas, and laser pulses as well as nozzle configuration on the cluster formation are studied. For the current experiments the laser ablation cluster source was optimized for production of Co_n^+ cluster ions. Clusters with n up to 150 atoms are registered by a time-of-flight mass spectrometer. Deposition of size-selected Co_{50}^+ clusters with kinetic energies in the interval of 250–4850 eV/cluster on highly ordered pyrolytic graphite is studied. At the highest impact energies the clusters are implanted. Craters and well-like structures can be seen by scanning tunneling microscopy at impact spots. A decrease in cluster kinetic energy leads to formation of bumplike structures which probably represent damaged graphite areas with incorporated Co atoms. Further decrease in the cluster impact energy to the level of 450–250 eV/cluster creates condition for so-called cluster pinning when the cluster constituents are intact but the energy transferred to the graphite is still enough to produce radiation defects to which the cluster is bound. © *2008 American Institute of Physics.* [DOI: 10.1063/1.2952503]

I. INTRODUCTION

In the last decade, the possibility of designing and mastering the physical and chemical properties of nanostructured materials has led to considerable interest and activity both in research and industry. Size reduction effects on the electronic, magnetic, optical, and some other properties in nanometric systems are key parameters that can to some extent be modified and controlled to meet technological requirements. Fundamental study is an important aspect to approach practical applications of nano-objects.

Cluster ion beams are efficient tools for manipulating agglomerates of atoms providing control over the synthesis of structures on the nanometer scale, in particular, control of cluster [nanoparticle (NP)] size and interaction energy with the substrate.[1–4] Cluster beams can also be utilized for formation of ordered arrays on patterned or functionalized surfaces.[5,6] One of the main advantages of the cluster ion beam technique, compared to some other methods such as chemical preparation[7,8] or atomic vapor growth of NPs,[9] is precise control of the cluster impact energy, high cluster size resolution, and easy fabrication of very small clusters consisting of just a few or few tens of atoms having sizes below or on the level of 1 nm. NPs of this size are of great interest due to the quantum confinement effects leading to extraordinary properties. For instance, isolated metal clusters deposited and adsorbed on a surface retain enhanced orbital and spin moments relative to the bulk.[10] Deposited or encapsulated Co and Fe clusters demonstrate high uniaxial magnetic anisotropy which can be controlled by changing the electronic properties of the matrix surrounding the clusters.[11] Recently, it was shown that the highest enhanced magnetic field response of spin-dependent transport can be reached in the case of very small Co clusters (15 atoms mean size) embedded in a thin copper layer.[12] Clusters of transition metals can also be proposed as catalysts for controllable growth of single-walled carbon nanotubes. Their typical diameters vary around 1.0–1.5 nm. It is suggested that precisely defining the catalyst diameter for the above-mentioned size range may be a key factor to control the structure and properties of the growing tube.

There are several methods for cluster beam production.[2,3] Among them, the widely used approaches to produce clusters are by gas aggregation, surface erosion, and in electrosprays. In the family of surface erosion cluster sources, the laser ablation technique has become one of the most popular owing to its applicability to a wide range of materials.[13] However, the performance of such cluster sources is dependent on many parameters. This article describes in detail the design and performance of a newly built laser ablation cluster source (LACS) which is connected to an existing cluster implantation and deposition apparatus (CIDA).[14] Test experiments on cluster beam optimization and control and first results on energetic deposition of mass-selected cobalt clusters are reported.

II. EXPERIMENTAL SETUP

A. Laser ablation cluster source

The design of our cluster source is similar to one that was first reported in Ref. 15. A schematic of the source can

[a]Electronic mail: sasa.vuckovic@physics.gu.se.
[b]Also at Fakultät für Physik, Universität Freiburg, D-79104 Freiburg, Germany.

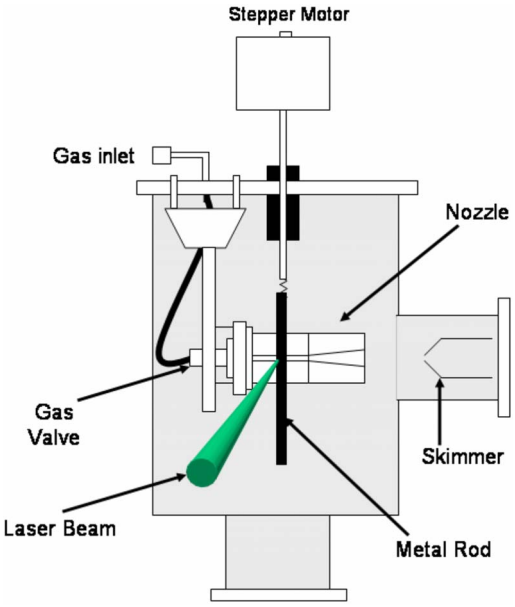

FIG. 1. (Color online) Schematic of the vacuum chamber containing the laser ablation source (not to scale).

be seen in Fig. 1. The cluster source is mounted on an ISO-K 250 flange inside a cylindrical vacuum chamber which is evacuated by a turbomolecular pump (Pfeiffer, 520 l/s) backed by a rotary vane pump. A base pressure of 1×10^{-6} Torr is provided. The chamber has ports for windows and pressure gauge as well as a CF100 port to be connected to the CIDA.

The main part of the source is the ablation cell that has a cubic shape ($30\times30\times30$ mm^3) and is made of stainless steel. There are three crossed channels drilled through the cell. The vertical through channel (6 mm in diameter) is designed for a metal rod used for ablation. Any kind of material prepared as a 6 mm rod can be used to produce clusters by laser vaporization. The rod is connected through a rotary feedthrough to a stepper motor mounted outside on the ISO-K 250 flange. The stepper motor provides rotational and translational (up and down) motion of the rod, in order to ensure a fresh spot for the ablation by every laser pulse as well as homogenous erosion of the rod.

The vertical channel is crossed by a horizontal one (2 mm in diameter) for the incoming laser pulse used to ablate the rod. The second horizontal channel (2 mm in diameter) intersects both channels and serves to mix the ablated material with a carrier gas and steer it towards the nozzle. On one end of this channel a solenoid valve (Parker General), providing pulses of a carrier gas (He in our case), is mounted. The gas injected into the channel is mixed with the ablated metal vapor. It cools the vapor and steers it towards the other end where the nozzle is mounted. Four different nozzles were used. More detailed analysis on the nozzle shape can be found below. Supersonic expansion of the vapor through the nozzle leads to cluster beam formation. The cluster beam is further collimated by the skimmer which has an opening of 3 mm in diameter and is located 5 cm behind the nozzle outlet.

The second harmonic (532 nm) of a Nd:YAG (yttrium aluminum garnet) laser (Quantel Brilliant) with a pulse duration of 5 ns operating at 20 Hz is used to ablate the rod. The laser beam is steered toward a kodial viewport which has over 90% transparency for 532 nm and focused through the first horizontal channel of the ablation cell on to the rod with a spot of approximately 1 mm in diameter. The laser pulses are synchronised and delayed with respect to the pulses of carrier gas. This procedure will be described in more detail below.

B. Cluster implantation and deposition apparatus

To detect, characterise and deposite the metal clusters, LACS is attached to the existing ultrahigh vacuum (UHV) setup called CIDA which is described in detail elsewhere.[14] This apparatus has been used to study energetic cluster-surface collisions utilizing another cluster source PuCluS.[16–18] Since the apparatus was designed to be universal, it can be used in connection to both sources. Figure 2 shows attachment of the sources to the acceleration chambers of the CIDA. One should note, that LACS is connected to CIDA through a flexible bellow in such a way that its main axis is deflected with respect to the main axis of the acceleration chamber by about 10 degrees. This connection allows the separation of the positively charged clusters which will be steered along the main axis of the acceleration chambers from the negatively charged or neutral clusters which will continue along the main axis of LACS thus colliding with the walls of the acceleration chambers. There is also a pneumatic gate valve between the LACS and acceleration chambers in order to be able to separate them.

The design of the acceleration chambers were slightly changed compare to that described in Ref. 14. It consists of two sections now. However they contain the same parts, namely, grids of the time-of-flight (TOF) mass spectrometer in Wiley–McLaren configuration, two Einzel lenses to focus a beam of positively charged clusters, two pairs of deflectors to steer the beam in vertical and horizontal directions, mass-selector and the postacceleration cylinder. There are some small constructive changes made compared to the earlier version that improved the performance of the steering, mass selection, and acceleration.

In particular, there is the possibility to ionise neutral clusters, which represent a majority of the clusters produced by laser ablation, thus increasing the intensity of the positively charged cluster beam. To perform the ionization, the beam of an excimer ArF laser with wavelength of 193 nm (6.4 eV) is steered between the first two grids of the TOF mass spectrometer perpendicular to the direction of the cluster beam coming from the source. It was found that the ionization potential is below 6.4 eV for Cu, Co, Fe, Nd, and Ni clusters starting from $n=3$.[19–22] Thus our excimer laser can be used for postionisation of clusters of these metals starting from trimmers as well as slightly larger clusters of some other metals: Au, Pd, Pt, etc.

The ionized clusters can be size selected with a resolution of $n/\Delta n\approx100$ using the gate which consists of a grid with large cells. The gate is closed by a high voltage which is continuously applied apart from a short controlled time (on

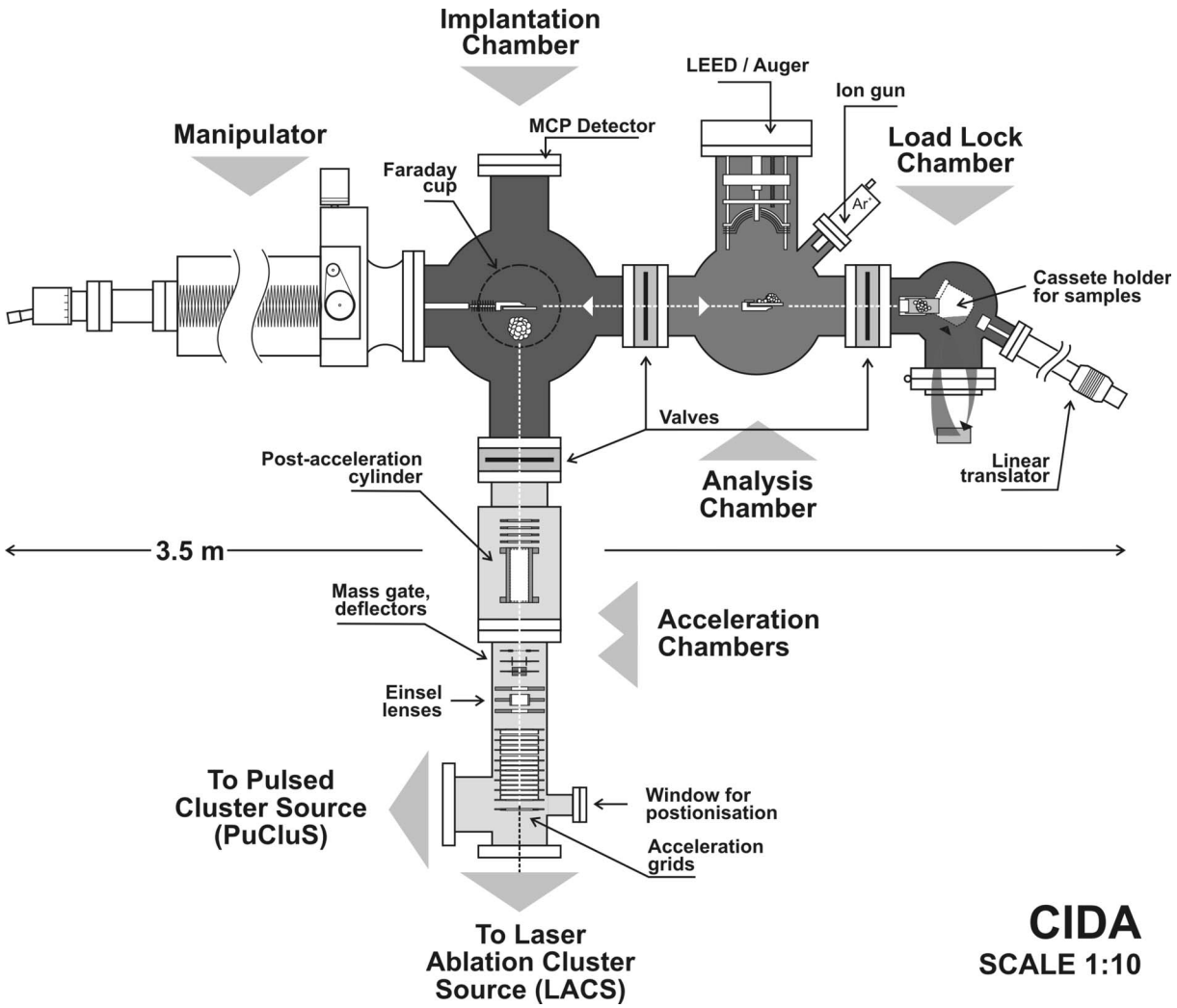

FIG. 2. Schematic of CIDA.

microsecond scale) when the clusters of desired size can pass through.

III. OPTIMIZATION OF LACS FOR COBALT CLUSTER PRODUCTION

The cluster production by laser ablation is determined by many interrelated parameters. An improper choice of these parameters may lead to no cluster formation while the optimization and synchronization can provide a range of cluster sizes with considerable intensity of the cluster beam. Pressure of the carrier gas, duration of the gas pulse, synchronization of this pulse with the flash lamp of the laser and the following synchronization of the pulses applied to the grids of the TOF spectrometer (acceleration grids) and the size-selection gate as well as the laser power are among the most important parameters. The source was optimized for the production of Co_n^+ cluster ions.

A. Synchronization of trigger pulses

The trigger pulses are produced and controlled using digital delay generators (Stanford). Figure 3 shows the order in which the signals are produced. The initial triggering pulse is sent as a gate signal to the gas valve driver (Parker) opening the solenoid valve (Pneutronics) for 800 μs in the present experiments, letting the carrier gas fill the ablation cell. A delayed signal is then sent to the ablation laser, triggering the flashlamp. The Q switching occurs after a default 285 μs delay after the flashlamp, producing the laser pulse. A triggering pulse is then sent to the high voltage switches connected to the grids of the TOF spectrometer. If additional ionization is used, this pulse is also sent as a triggering pulse to the excimer ArF laser. For mass selection and postacceleration, subsequent triggering pulses are sent to the corresponding high voltage switches. By postacceleration the cluster energy can be increased up to 20 keV but this option is not used in the current experiments and therefore is not further discussed. All delay times can be separately controlled using the delay generators. The frequency used in this setup is 20 Hz, which is the pulse frequency allowed for the ablation laser.

B. Optimization of delay times

To find the dependence of mass distribution on the delay time between the gas valve opening and the ablation laser pulse, a number of mass spectra have been recorded for several different delay times and pressures of the carrier gas.

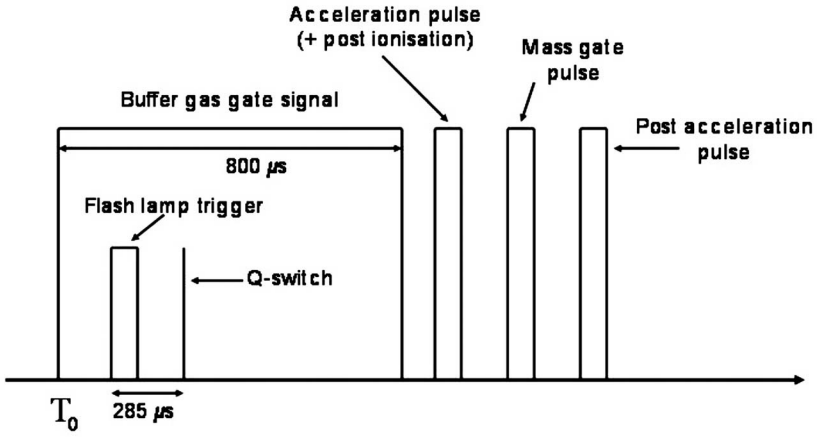

FIG. 3. The order of the trigger and gate signals for the main mechanism of the creation and control of the cluster ion beam.

Figure 4 shows four mass distributions for different delay times at fixed gas pressure. For short delay times, the intensities are low and small clusters dominate. As the delay time increases, both the intensity and the average cluster size increases until a certain delay value when they start decreasing and further difference in delay time of a few tenths of microseconds leads only to the monomer and dimer production. The optimal delay times are found to be around 600 μs.

The low intensities of large clusters at small delay times are related to the case when the ablation pulse arrive too early, before the carrier gas reaches the stagnation pressure value in the ablation cell. As soon as the delay time is increased and the stagnation value is reached, the nucleation of small cluster "seeds" is optimized by the He cooling. A three-body collision between two ablated Co atoms and one He atom is needed in order to remove excess energy and nucleate a small cluster. This type of collision is facilitated in dense vapor. The stabilized He pressure also cools hot large clusters more efficiently, thus preventing their fragmentation. As a result, the mass spectrum contains larger cluster sizes and higher intensity. The increase of the delay time over 650 μs at fixed duration of the gas pulse of 800 μs reduces the time during which the cluster nucleation is possible and therefore leads to the decrease in the cluster beam intensity. The delay time and duration of the pulse for the acceleration grids were optimized by varying these parameters in order to maximize the response from the detector. The delay and pulse duration times applied to the mass gate were found in a similar way.

C. Carrier gas pressure and nozzle shape

The pressure inside the ablation cell affects a number of processes: development of the laser ablation plume, the efficiency of the hot vapor cooling, the cluster condensation, and the nozzle expansion dynamics. Figure 5 shows a series of mass spectra for different backing pressures of the carrier gas. As can be seen, the pressure has no significant effect on the mass distribution in the range between 8 and 10 bars, even though a small increase in intensity of the higher mass peaks can be observed for higher pressures. However, it should be considered that the detection efficiency of the detector drops for the larger clusters. There is however a large difference in the mass distribution comparing higher pressures with lower pressures. As the backing pressure decreases the mass distribution shifts to lower cluster sizes, and at 5 bars the mass cluster peaks almost disappear.

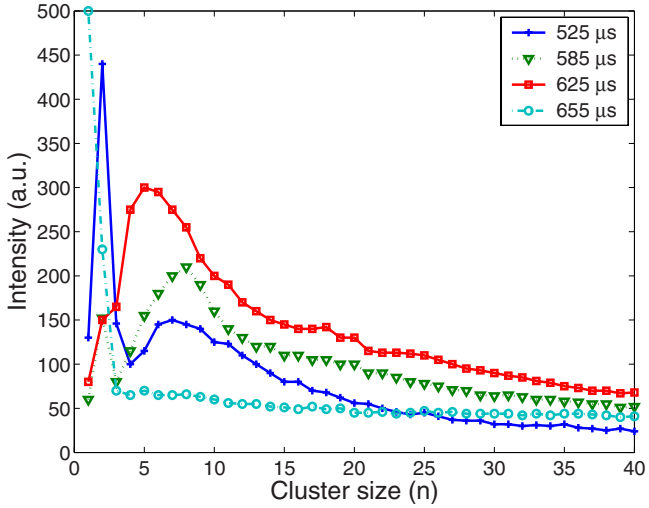

FIG. 4. (Color online) Cluster size distribution for different delay times between the opening of the gas valve and the laser pulse at constant carrier gas pressure of 7 bars.

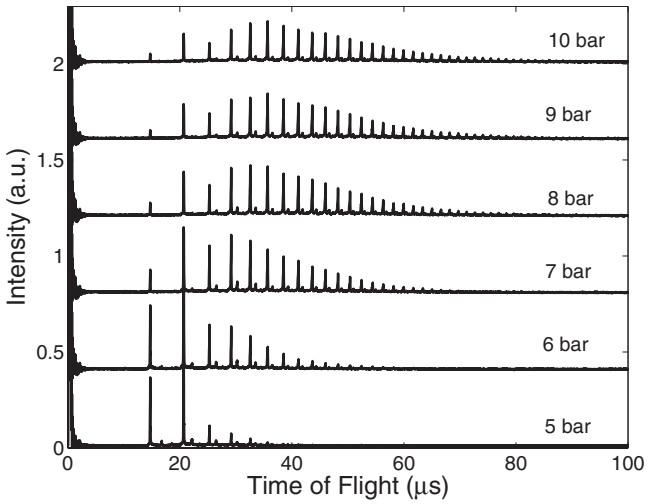

FIG. 5. Mass spectra of Co_n^+ cluster ions for different carrier gas pressures and other parameters kept constant.

These results can be interpreted in terms of the scaling law for gas condensation under supersonic expansion proposed in Refs. 23 and 24. With the other parameters fixed, this scaling law suggests that the average cluster size is a linear function of the number density of the constituents which is proportional to the gas backing pressure. However, one should remember that in our case we do not have a pure gas supersonic expansion but it is combined with the ablation process. The expansion of the hot vapor from the ablation plume in an ambient gas can be described as an expanding jet[25] also following the scaling law. In the present case, the backing pressure has to be substituted by the stagnation pressure in the ablation cell since there is a large flow through the laser entrance channel. Thus, we have two processes—expansion into vacuum and vapor expansion after laser ablation—that follow the scaling law but have radically different parameters. On the one hand, higher stagnation pressure should lead to the formation of larger clusters in the supersonic jet but on the other hand, the increase in the stagnation pressure over a certain value starts suppressing the development of the ablation plume. The detailed study of these processes is out of the scope of present paper. However one should notice that some compromise in pressure must be reached in order to facilitate both processes which is found to be between 8 and 10 bars in our setup.

The cluster formation also significantly depends on the nozzle shape which affects the gas flow and atomic collisions on expansion. Four different nozzles have been tried. One is a sonic capillary nozzle with a diameter of 1 mm giving a very fast expansion. The other three are conical nozzles with the same orifice of 1 mm, length of 30 mm but different opening angles to the beam axis of 8°, 10°, and 15°. It was found that the conical nozzle with an angle of 8° gives by far the best intensities. The sonic capillary nozzle gives low intensities for higher masses compared to the conical nozzles.

D. Optimization of laser power

One more important parameter that influences the cluster formation is the power of the laser pulse. The laser beam is focused on the target into the spot of about 1 mm in diameter. Interaction of the laser pulse with the rod material leads to vaporization of a small surface region and formation of a plume of hot plasma. The ablation process depends on many different parameters which are subjects of independent studies. More details can be found, for instance, in Refs. 3 and 25–27. In Fig. 6 one can see how the cluster size distribution and intensity depend on the laser power in our case. At low power values the amount of the vaporized material is small, leading to formation of small clusters. The increase in power to 20–30 mJ/pulse produces a pretty wide size distribution with considerable intensity. This power window is found to be optimal for our cluster source. Further increase in power leads to the ablation of relatively large amounts of material. Since the time scale for the development of the ablation plume is shorter than the laser pulse duration, this vaporized material starts absorbing the laser light thus shielding the target. Hence, a significant decrease of the cluster beam intensity is observed, see, for instance, the curve corresponding to 58 mJ in Fig. 6.

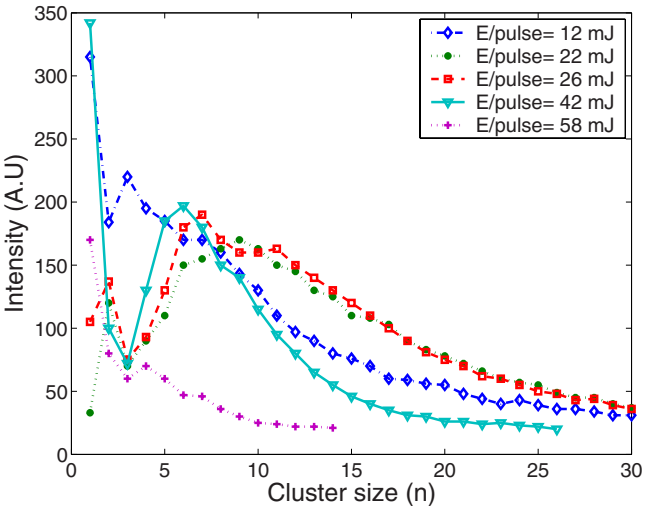

FIG. 6. (Color online) Cluster size distributions for different laser powers and other parameters kept constant.

A typical mass spectrum of Co_n^+ cluster ions obtained after optimization of the source parameters is presented in Fig. 7. The spectrum is recorded for the case when the cluster ions were accelerated to 3.2 keV. Clusters up to 150 atoms in size can be resolved. The decrease in intensity of heavy clusters is related not only to drop of their ratio in the beam but also to the lower efficiency of the detector to register larger charged particles. Mean cluster sizes (diameters D) presented in Fig. 7 are estimated using spherical cluster approximation

$$D = 2R_{\mathrm{WS}}(n/f)^{1/3}, \tag{1}$$

where R_{WS} is the Wigner–Seitz radius for Co and f is the packing factor assumed to be equal to 0.74 (typical for icosahedral, bcc and fcc structures).

IV. DEPOSITION OF COBALT CLUSTERS

One can expect different behavior of the deposited clusters depending on the size and impact (kinetic) energy. If

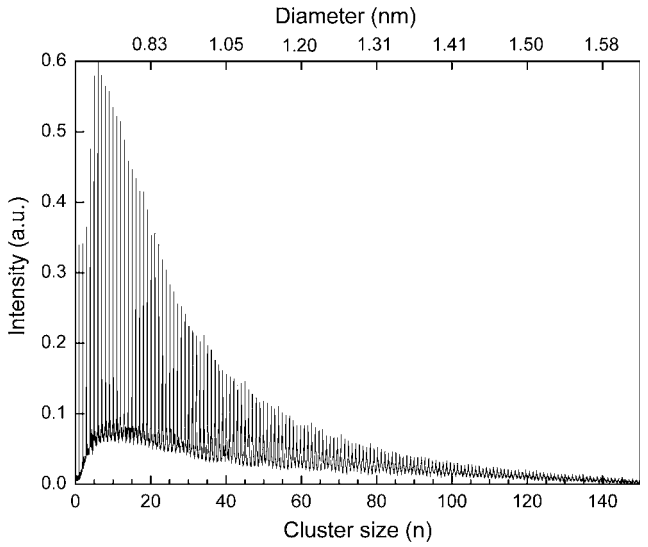

FIG. 7. Mass spectrum of Co_n^+ cluster ions obtained after optimization of source parameters.

clusters of all sizes are accelerated to the same energy, for instance, of a few hundreds of eV, then the smallest clusters will be destroyed on impact and their constituents will be implanted because their binding energies are much lower compared to the kinetic energy per atom. The kinetic energy per atom of the largest clusters can be smaller than the binding energy per atom that will lead to soft landing. However, in the case of soft landing significant changes in cluster morphology often take place due to surface mobility, diffusion, and aggregation. That is a negative effect which ruins the advantage of size selection for practical applications. An intermediate behavior can be expected for the medium size clusters when their kinetic energies per cluster atom are comparable with the binding energies. On the one hand, a cluster can preserve its composition on impact but, on the other hand, the density of the deposited energy can be already high enough (because of significant number of atoms transferring the energy to the substrate at the same impact spot) to replace one or a few substrate atoms producing a radiation defect to which the cluster can be bound. This case corresponds to so-called cluster pinning which was found both experimentally and theoretically for different cluster species.[28–30] The pinned clusters are deformed in shape on impact but they keep their size and they are immobilized on the surface.

In order to predict the cluster behavior on deposition it is important to compare the kinetic energies with binding energies of atoms in clusters. However, to our knowledge there are no experimental data on this subject for Co clusters, which are used for the deposition in current experiments, excepting the measurements of the dissociation energy of Co dimer which was found to be 1.74 ± 0.26 eV.[31] The theoretical simulations are quite controversial. It was predicted that the binding energy of very small ($n=2-5$) Co clusters can vary between 1.15 and 4.45 eV/atom.[32] Other simulations present a rather different energy interval of 0.43–0.98 eV/atom for the same sizes.[33] Recent calculations show that the binding energy of neutral cobalt clusters increases with size and reaches ~3.8 eV/atom for $n=13$.[34] On the other hand, simulations presented elsewhere show that the binding energy significantly depends on the cluster packing and for $57 \leqslant n \leqslant 177$ it varies between 1.6 and 2.0 eV/atom.[35] Nevertheless, most of the computer simulations agree on the tendency for binding energy to increase with size. However, this tendency rapidly slows down already for sizes of a few tens of atoms. For instance, it is found for Al clusters that the binding energy increases only by about 4% with an increase in size from 52 to 102 atoms.[36]

For the first series of experiments size-selected $Co_{50\pm5}$ clusters were chosen. They were deposited on a freshly cleaved surface of highly ordered pyrolitic graphite (HOPG) in a vacuum of $(2-3)\times10^{-9}$ Torr. Kinetic energies varied from 250 to 4850 eV/cluster (mean energy from 5 to 97 eV/atom). The HOPG surfaces with the deposited clusters were studied using scanning tunneling microscopy (STM) in the constant current mode with the bias of 0.1 V. The used instrument was Ntegra–Aura (NT-MDT). Figure 8(a) shows the HOPG surface bombarded by the clusters with the highest chosen energy. One can see the formation of

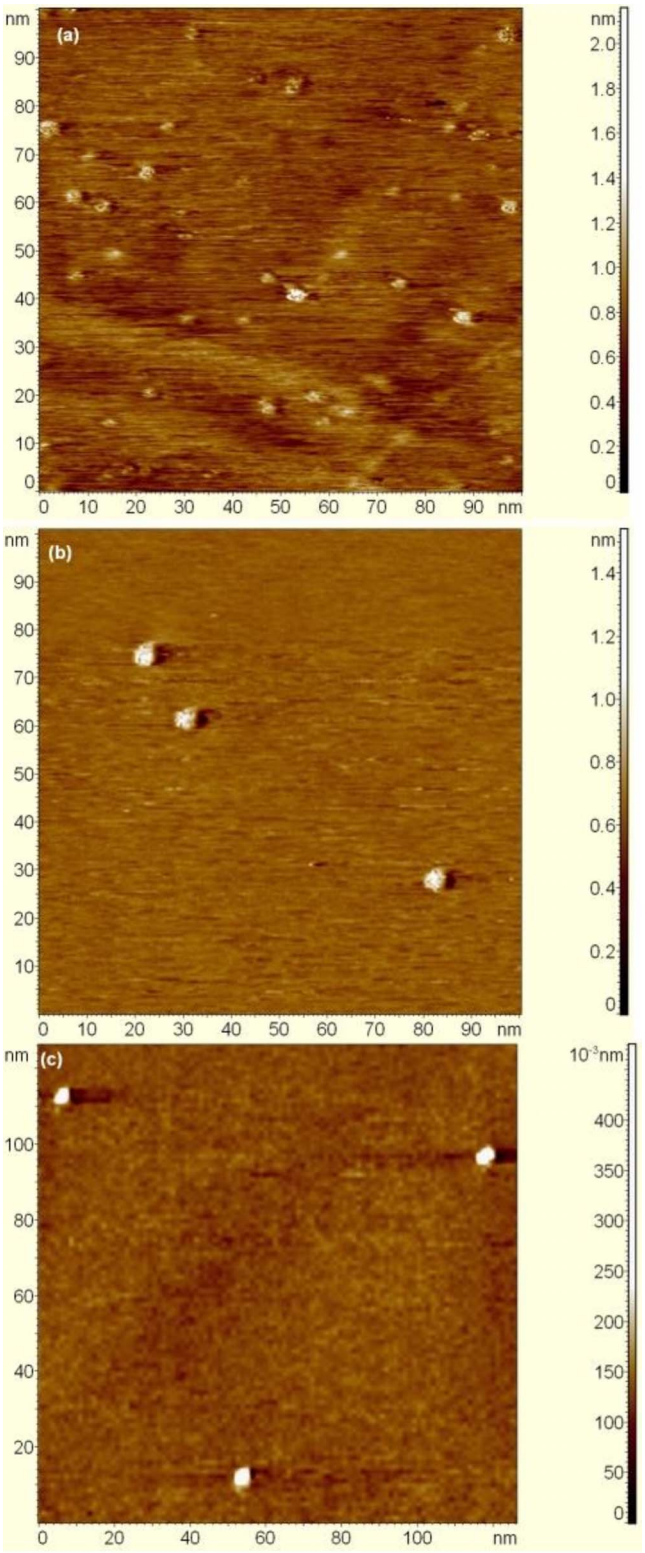

FIG. 8. (Color online) STM images of $Co_{50\pm5}$ clusters deposited on HOPG with energies of: (a) 4850 eV/cluster, (b) 1500 eV/cluster, and (c) 450 eV/cluster.

radiation damaged areas which are about 2.0–2.5 nm in diameter and 0.35–0.40 nm in height. In most cases an impact spot looks like a partly filled crater or well. In some cases one can clearly see a centrally positioned bump in a crater. Crater formation is quite possible for this cluster size and energy. For example, it was shown elsewhere[37] that the im-

pact of 5–6 keV Ar_{12} or Ar_{43} clusters on graphite leads to a small crater opening in the early phase of the collision cascade but the crater can partly recover (close) at later stages because of the relaxation of the damaged graphite layers. These observed structures are also consistent with the earlier predicted case for the implantation of Ag_{147} clusters into HOPG when the clusters come to rest at the bottom of an open well produced by the impact, thus filling it.[38] Similar effect was observed on impact of Au_n (n is from 13 to 402) clusters with graphite at fixed energy of 100 eV/atom.[39]

A decrease in the kinetic energy to 1500 eV/cluster (30 eV/atom) leads to the formation of damaged areas with mean diameter of about 3 nm [Fig. 8(b)]. Here the bumps are slightly higher, ~0.45 nm and they are more symmetric in shape. The energy is too low to form craters or wells. These bumps most probably represent intermixture of the cobalt atoms from the broken clusters and carbon atoms displaced on the cluster impact.

Further reduction in the mean kinetic energy to 20 and then to 12 eV/atom leads to a decrease in the damaged area diameters to ~2 nm. They also become slightly lower in height, 0.4 nm. The images obtained on the samples after the cluster deposition with energies of 450–250 eV/cluster (9, 7, 6, and 5 eV/atom) look very similar to each other and a typical one is shown in Fig. 8(c). The bump diameters are 1.4–1.5 nm and their mean height is 0.3 nm. It was suggested in Ref. 28 that cluster pinning occurs when the cluster provides enough energy E_T to produce the recoil carbon atom. The developed analytical model yields the result for the threshold pinning energy

$$E_{\text{pin}} = nM_e \frac{E_T}{4M_C}, \tag{2}$$

where n is the number of atoms in the cluster, M_e is the atomic mass of the chemical element composing the cluster, and M_C is the atomic mass of the target atoms which is carbon in our case. Equation (2) predicts E_{pin}=5.7 eV/atom for cobalt clusters on HOPG. Thus, the above mean energy "window" of 5–9 eV/atom can correspond to pinning of the cobalt clusters in our case. Note that if one compares the samples corresponding to 250 and 350 eV/cluster, which have almost equal deposition times, the surface density of the deposited clusters found by STM is significantly lower for the 250 eV/cluster energy compared to the 350 eV/cluster one. This is most probably the consequence of the wide interval of cluster sizes selected for the deposition, from 45 to 55 atoms, i.e., for the case of 250 eV/cluster the energy per atom varies from 5.5 to 4.5 eV, correspondingly. Hence, only the smallest clusters are pinned while the larger clusters are soft landed and they diffuse to surface defects, for example, to nearest graphite steps and become unresolved by STM. Comparison of the images corresponding to 350 and 450 eV/cluster deposition energies shows a similar surface density of the deposited clusters. However, the deposition time for the later sample was about two times lower. Thus, we still have a significant number of not pinned clusters for the 350 eV/cluster energy that corresponds to the interval of 6.4–7.8 eV/atom. From the above considerations one can conclude that the energy interval for the pinning threshold varies between ~5.0 and 7.0 eV/atom which is in good agreement with the theoretical prediction. Although these energies are higher that the calculated binding energies, the STM shows that the pinned clusters are still intact but flattened because their heights are four to five times smaller than the diameters.

V. CONCLUSIONS

A source utilizing laser ablation of material for production of atomic clusters is described. The influence of various source parameters such as carrier gas pressure, laser power, delay time between the gas and laser pulses as well as nozzle configuration on the cluster formation is studied. These parameters are optimized for the production of Co_n^+ cluster ion beams. The source is connected to an apparatus that allows control of the cluster size and kinetic energy and utilizes the cluster beam for deposition or implantation experiments under UHV conditions.

The size-selected $Co_{50\pm5}^+$ cluster ions are used for a first series of deposition/impact experiments on HOPG surface. It is shown that the cluster impacts with energy of 4.85 keV/cluster originate small (2.0–2.5 nm in diameter) damage areas on the surface. One can resolve a partly filled craters or wells using the STM. Decrease of the cluster impact energy to 1.5 keV/cluster leads to conversion of crater-like structures into bumps. The energy is too low to form the craters. These bumps most probably represent the intermixture of cobalt atoms from the broken clusters and carbon atoms displaced on the impact. Under further decrease in the cluster impact energy to 250–450 eV/cluster one can observe very small (~1.4 nm in diameter and ~0.3 nm in height) bumps. According to the cluster pinning model introduced elsewhere,[30] it is possible to suggest that the above interval of energies, which correspond to 5–9 eV/atom, can correspond to pinning of the $Co_{50\pm5}$ clusters. Thus, the observed bumps are the deposited clusters flattened on impact. The study of the metal cluster impact especially of the pinning regime depending on the cluster size and type of substrate will be continued.

ACKNOWLEDGMENTS

The financial support of the Swedish Research Council under the Project No. 621-2005-6272 is acknowledged. Two of the authors (S. V. and V. N. P.) are also grateful for the support of the Nanoparticle Platform at the Science Faculty of the University of Gothenburg.

[1] W. Habrich, *Metal Clusters at Surfaces*, edited by K. H. Maiwess-Broer (Springer, Berlin, 2000), p. 107.
[2] K. Wegner, P. Piseri, H. Vahedi Tafreshi, and P. Milani, J. Phys. D: Appl. Phys. **39**, R439 (2006).
[3] V. N. Popok and E. E. B. Campbell, Rev. Adv. Mater. Sci. **11**, 19 (2006).
[4] R. E. Palmer, S. Pratontep, and H.-G. Boyen, Nat. Mater. **2**, 443 (2003).
[5] L. Bardotti, B. Prevel, P. Jensen, M. Treilleux, P. Melinon, A. Perez, J. Gierak, G. Faini, and D. Mailly, Appl. Surf. Sci. **191**, 205 (2002).
[6] U. Queitsch, E. Mohn, F. Scaffel, L. Schultz, B. Rellinghaus, A. Bluher, and M. Mertig, Appl. Phys. Lett. **90**, 113114 (2007).
[7] J. P. Wilcoxon, J. E. Martin, and P. Provencio, J. Chem. Phys. **115**, 998 (2001).
[8] K. C. Grabar, R. G. Freeman, M. B. Hommer, and M. J. Natan, Anal. Chem. **67**, 735 (1995).

[9] B. Bennewitz, J. N. Crain, A. Kirakosian, J.-L. Lin, J. L. McChesney, D. Y. Petrovykh, and F. J. Himpsel, Nanotechnology **13**, 499 (2002).
[10] C. Binns, K. N. Trohidou, J. Bansmann, S. H. Baker, J. A. Blackman, J.-P. Bucher, D. Kechrakos, A. Kleibert, S. Louch, K.-H. Meiwes-Broer, G. M. Pastor, A. Perez, and Y. Xie, J. Phys. D: Appl. Phys. **38**, R357 (2005).
[11] F. Luis, F. Bartolom, F. Petroff, J. Bartolom, L. M. Garca, C. Deranlot, H. Jaffrs, M. J. Martnez1, P. Bencok, F. Wilhelm, A. Rogalev, and N. B. Brookes, Europhys. Lett. **76**, 142 (2006).
[12] S. Serrano-Guisan, G. Di Domenicantonio, M. Abid, J.-P. Abid, M. Hillenkampi, L. Gravier, J. P. Ansermet, and Ch. Felix, Nat. Mater. **5**, 730 (2006).
[13] M. Pellarin, E. Cottancina, J. Lerma, J. L. Viallea, J. P. Wolfa, M. Broyera, V. Paillardb, V. Dupuisb, A. Perezb, J. P. Perezb, J. Tuaillonb, and P. Melinonb, Chem. Phys. Lett. **224**, 338 (1994).
[14] V. N. Popok, S. V. Prasalovich, M. Samuelsson, and E. E. B. Campbell, Rev. Sci. Instrum. **73**, 4283 (2002).
[15] R. E. Smalley, Laser Chem. **2**, 167 (1983).
[16] V. N. Popok, S. V. Prasalovich, and E. E. B. Campbell, Nucl. Instrum. Methods Phys. Res. B **207**, 145 (2003).
[17] S. Prasalovich, V. N. Popok, P. Persson, and E. E. B. Campbell, Eur. Phys. J. D **36**, 79 (2005).
[18] J. Samela, K. Nordlund, J. Keinonen, V. N. Popok, and E. E. B. Campbell, Phys. Rev. B **77**, 075309 (2008).
[19] M. B. Knickelbein, S. Yang, and S. J. Riley, J. Chem. Phys. **93**, 94 (1990).
[20] S. Yang and M. B. Knickelbein, J. Chem. Phys. **93**, 1533 (1990).
[21] M. B. Knickelbein, Chem. Phys. Lett. **192**, 129 (1991).
[22] M. B. Knickelbein and S. Yang, J. Chem. Phys. **93**, 5760 (1990).
[23] O. F. Hagena and W. Obert, J. Chem. Phys. **56**, 1793 (1972).
[24] O. F. Hagena, Z. Phys. D: At., Mol. Clusters **4**, 291 (1987).
[25] A. V. Bulgakov and N. M. Bulgakova, J. Phys. D: Appl. Phys. **31**, 693 (1998).
[26] H. Hsieh, R. S. Averback, H. Sellers, and C. P. Flynn, Phys. Rev. B **45**, 4417 (1992).
[27] S. Gibilisco, M. Di Vece, S. Palomba, and G. Faraci, J. Chem. Phys. **125**, 084704 (2006).
[28] S. J. Carrol, S. Pratontep, M. Streun, R. E. Palmer, S. Hobday, and R. Smith, J. Chem. Phys. **113**, 7723 (2000).
[29] M. Di Vece, S. Palomba, and R. E. Palmer, Phys. Rev. B **72**, 073407 (2005).
[30] R. Smith, C. Nock, S. D. Kenny, J. J. Belbruno, M. Di Vece, S. Palomba, and R. E. Palmer, Phys. Rev. B **73**, 125429 (2006).
[31] A. Kant and B. Strauss, J. Chem. Phys. **41**, 3806 (1964).
[32] M. Castro, C. Jamorski, and D. R. Salahub, Chem. Phys. Lett. **271**, 133 (1997).
[33] M. Pereiro, S. Man'kovsky, D. Baldomir, M. Iglesias, P. Mlynarski, M. Valladares, D. Suarez, M. Castro, and J. E. Arias, Comput. Mater. Sci. **22**, 118 (2001).
[34] Q.-M. Ma, Z. Xie, J. Wang, Y. Liu, and Y.-Ch. Li, Phys. Lett. A **358**, 289 (2006).
[35] R. Guirado-Lopez, F. Aguilera-Granja, and J. M. Montejano-Carrizales, Phys. Rev. B **65**, 045420 (2002).
[36] J. Akola, M. Manninen, H. Hkkinen, U. Landman, X. Li, and L.-Sh. Wang, Phys. Rev. B **62**, 13216 (2000).
[37] J. Samela, K. Nordlund, J. Keinonen, V. N. Popok, and E. E. B. Campbell, Eur. Phys. J. D **43**, 181 (2007); J. Samela and K. Nordlund, personal communication (Nov. 19, 2007).
[38] S. J. Carrol, P. D. Nellist, R. E. Palmer, S. Hobday, and R. Smith, Phys. Rev. Lett. **84**, 2654 (2000).
[39] C. Anders and H. M. Urbassek, Nucl. Instrum. Methods Phys. Res. B **228**, 57 (2005).